PROCEEDINGS

FIRST VATICAN COFFIN CONFERENCE

19-22 JUNE 2013

VOLUME 1

VATICAN COFFIN PROJECT
Reparto Antichità Egizie e del Vicino Oriente
Laboratorio di Diagnostica per la Conservazione ed il Restauro

THANKS TO **Massachusetts Chapter**
Patrons of the Arts
in the Vatican Museums

Edited by
Alessia Amenta and Hélène Guichard

Scientific Text Editing
Mario Cappozzo, Agnese Iob

Photo Credits
Photos © Governatorato SCV, Direzione dei Musei
Images and Rights Office: Rosanna Di Pinto, Filippo Petrignani
Secretary for Departments: Daniela Valci, Gianfranco Mastrangeli
Photographers: Pietro Zigrossi, Alessandro Bracchetti, Giampaolo Capone, Luigi Giordano, Danilo Pivato, Alessandro Prinzivalle
All the other references are indicated in the photo credits list at the end of the book.

Graphic Design and Pagination
Giulia Angelini

Printing
Tipografia Vaticana

ISBN 978-88-8271-404-8 (2 volumes not to be sold separately)

Front and rear cover images:
Coffin lid of Djedmut and details, inv. MV25008
(photo by Danilo Pivato, © Governatorato SCV, Direzione dei Musei)

LOUVRE

MUSEI VATICANI

Rijksmuseum van Oudheden

PROCEEDINGS
FIRST VATICAN COFFIN CONFERENCE

19-22 JUNE 2013

VOLUME 1

edited by **ALESSIA AMENTA** and **HÉLÈNE GUICHARD**

EDIZIONI MUSEI VATICANI

CONTENTS

Volume 1

Foreword
ALESSIA AMENTA 15

MOHAMED I. ABOUELATA, MANAL A. HOSSIN
Continuity of themes depicted on coffin lids from Third Intermediate Period to Graeco-Roman Egypt 21

AVERIL ANDERSON, LUC BIDAUT
The Third Intermediate Period coffins in the McManus Museum, Dundee 31

MARIA VICTORIA ASENSI AMORÓS
The wood of the Third Intermediate Period coffins: The evidence of analysis for the *Vatican Coffin Project* 45

STEPHANIE D. ATHERTON-WOOLHAM, LIDIJA M. MCKNIGHT, JUDITH E. ADAMS, CAMPBELL PRICE
A scientific study of coffins in the Manchester Museum: Current and future work 51

FRUZSINA BARTOS
Cartonnage fragments from the 22nd Dynasty originating from Theban Tomb 65 and its surroundings 57

MARILINA BETRÒ
Birth, (re)-birth and votive beds: New evidence from a Third Intermediate Period context in Theban Tomb 14 63

ANDERS BETTUM
Nesting: The development and significance of the 'yellow coffin' ensemble 71

SUSANNE BICKEL
KV 64. An intact 22nd Dynasty burial in the Valley of the Kings. Preliminary description 83

FEDERICO BOTTIGLIENGO
Digging in the museum: Some notes on *Amduat* papyri in the Museo Egizio of Turin 89

GIACOMO CAVILLIER
The *Butehamun Project*: Research on the funerary equipment 97

KATHLYN M. COONEY
Coffin reuse: Ritual materialism in the context of scarcity 101

ALAIN DAUTANT, ALESSIA AMENTA
The coffins of Djedmut, Nurse of Khonsu the Child (Vatican, La Rochelle and Padua Museums) 113

ALAIN DAUTANT, MIGUEL ESCOBAR, FRANCE JAMEN
Distribution and current location of the French Lot from the Bab el-Gasus Cache 123

ALAIN DAUTANT, FRANCE JAMEN
Inventory of the 21st/22nd Dynasties 'yellow coffins' in French museums 129

CÁSSIO DE ARAÚJO DUARTE
The *Amduat* on the 21st Dynasty coffins 137

AIDAN DODSON
The Third Intermediate Period coffins in the collection of the Medelhavsmuseet, Stockholm 145

MONIKA DOLINSKA
The Third Intermediate Period coffins in the National Museum in Warsaw.
Presentation of the collection 155

SILVIA EINAUDI
The tomb of Padiamunipet (TT 33) and its role in the 'Saite recension' of the Book of the Dead 163

HÉLÈNE GUICHARD, SANDRINE PAGÈS-CAMAGNA, NOËLLE TIMBART
The coffin of Tanetshedmut of the Musée du Louvre: First study and restoration for
the *Vatican Coffin Project* 169

MARIA CRISTINA GUIDOTTI
Restoration works on coffins from the Late Period at the Museo Egizio of Florence 179

NADINE GUILHOU
Painters of coffins and papyri at Thebes in the Third Intermediate Period 183

EDOARDO GUZZON
The wooden coffins of the late Third Intermediate Period and Late Period found
by Schiaparelli in the Valley of the Queens (QV 43 and QV 44) 191

NESRIN M. M EL HADIDI, SAFA A. M. HAMED
The effect of preparation layers on the anatomical structure and chemical composition of native Egyptian wood 199

REMY HIRAMOTO
Terahertz (THz) imaging of 21st Dynasty coffins 211

FRANCE JAMEN
A textual-iconographical and technological study of unpublished 21st Dynasty coffins from Lyon: The coffins of *Pȝ-d(j)-ḥnsw* (Musée des Beaux-Arts, Invv. H 2320-H 2321) 219

CAROLA KOCH
The sarcophagus of Nitocris (Inv. Cairo TN 6/2/21/1): Further considerations about the God's Wives' burial places 231

ALEXANDRA KÜFFER
The coffins from the Cache-tomb of Bab el-Gasus in Switzerland 249

NIKA LAVRENTYEVA
The coffin of Padikhonsu from the Pushkin State Museum of Fine Arts, Moscow (Inv. 1, 1a 5316 / ИГ 5402) 255

ÉVA LIPTAY
The ancient Egyptian coffin as sacred space: Changes of the sacred space during the Third Intermediate Period 259

SABINA MALGORA, JONATHAN ELIAS
Symbolism in 21st Dynasty coffin art: Implications of the Trento coffin fragment (Inv. EMV 4517) 271

SABINA MALGORA, JONATHAN ELIAS
The coffin of Ankhpakhered (Inv. Asti 94a): Defining an Akhmimic regional style for the later Third Intermediate Period 277

LILIANE MANN
The letters of Willem Pleyte 289

LIDIJA M. MCKNIGHT, STEPHANIE D. ATHERTON-WOOLHAM, JUDITH E. ADAMS, CAMPBELL PRICE
Preliminary research on the Chester coffin. A potential case of mistaken identity and coffin reuse? 293

MARIA GRAZIA MIMMO
The beginning of the Third Intermediate Period 299

JULIE ANNE MORGAN
Image of the Sah: A study of the graphic styles and colour patterning on coffins dated from the 22nd to the 25th Dynasties 303

SUSANNA MOSER, GIAN LUIGI NICOLA
Sharing knowledge for restoring coffins: The case of Civico Museo di Storia e Arte of Trieste 317

MELINDA G. NELSON-HURST, JOHN W. VERANO
The Tulane University Egyptian collection: Reconstructing lost context – Phase 1 327

ANDRZEJ NIWIŃSKI
The 21st Dynasty coffins of non-Theban origin. A 'family' for the Vatican coffin of Anet 335

ELENA PAGANINI
Life and death of 'citizens' of Amun: A socio-economic investigation of the Bab el-Gasus Cache 349

SANDRINE PAGÈS-CAMAGNA, HÉLÈNE GUICHARD
Coloured materials of Theban coffins produced around the 'yellow coffin' series from the Louvre Collections 357

DANIELA PICCHI
The anthropoid coffin of Mesiset (?): An interesting history of collecting, typological study, and diagnostic investigation 361

LUIGI PRADA
A contribution to the textual and iconographical study of embossments from Third Intermediate Period mummy braces, chiefly from the Bab el-Gasus Cache and now in the Cairo Museum 369

Volume 2

GIOVANNA PRESTIPINO
The *Vatican Coffin Project*: Observations on the construction techniques of Third Intermediate Period coffins from the Musei Vaticani 397

NOEMI PROIETTI, VALERIA DI TULLIO, FEDERICA PRESCIUTTI, COSTANZA MILIANI, NICOLA MACCHIONI, DONATELLA CAPITANI
A 25th Dynasty coffin in the Museo del Vicino Oriente at Sapienza Università di Roma: A diagnostic multi-analytical study 407

MAARTEN J. RAVEN
Third Intermediate Period burials in Saqqara 419

NICHOLAS REEVES
The coffin of Ramesses II 425

ISABELLE RÉGEN
Tradition and innovation on the Third Intermediate Period coffins. The case of an uncommon rising solar and Osirian scene with hacking up of the earth 439

UTE RUMMEL, STÉPHANE FETLER
The coffins of the Third Intermediate Period from tomb K93.12 at Dra Abu el-Naga. Aspects of archaeology, typology, and conservation 451

GÁBOR SCHREIBER
The burial assemblages of Ankhefenamun and Hor, and other Third Intermediate Period burials from Theban Tomb -61- 463

IAN SHAW
New Kingdom and Third Intermediate Period coffin and textile remains from the 2011-2012 excavations at Medinet el-Gurob, Fayum region 471

CYNTHIA MAY SHEIKHOLESLAMI
Iconography and dating of some Vatican coffins (Museo Gregoriano Egizio, Invv. D 2067.6.1-6 and MV 25007) 483

RENATE SIEGMANN
The 'patchwork coffin' of the Servant (*sḏm ʿš*) of a High Priest of Amun-Re in the Musée d'ethnographie Neuchâtel (late 21st/early 22nd Dynasty) 503

LOREDANA SIST
A 25th Dynasty Theban coffin in the Museo del Vicino Oriente at Sapienza Università di Roma 509

ROGÉRIO SOUSA
Building catalogues. The concept of 'architectonisation' and the description of coffins of the 21st Dynasty 515

HELEN STRUDWICK
The enigmatic owner of the coffins of Nespawershefyt at the Fitzwilliam Museum, Cambridge 521

MYKOLA TARASENKO
The Third Intermediate Period coffins in the Museums of Ukraine 529

JOHN H. TAYLOR
The vulture headdress and other indications of gender on women's coffins in the 1st millennium BC 541

IGOR URANIC
The Third Intermediate Period mummies and the coffins from the Arheološki Muzej in Zagreb 551

RENÉ VAN WALSEM
The chain motif. A decorative architectonic element with prehistoric roots on the lid of some 'stola coffins' 557

Posters 575

Conference bursary 593

Bibliography 597

Index of museum numbers 685

Contributors 707

Remembering the conference... 716

The effect of preparation layers on the anatomical structure and chemical composition of native Egyptian wood*

Nesrin M. N. El Hadidi, Safa A. M. Hamed

Introduction

In ancient Egypt, preparation layers were used as a surface coating for wooden sculptures, funerary furniture such as coffins, boat models, boxes, statues, etc.., where it served as a ground for painting or gilding and also to suppress the wood defects and any unevenness of the surface. Preparation layers on wooden coffins, often referred to as ground layers in a lot of literature; vary in their composition and complexity. Stein and Lacovaranoted that the use of these layers, whether of mud, chalk or both, may improve long-term adhesion, and essentially cushions the brittle paint from the movement of the underlying wood.[1] Hatchfield and Newman's analyses of Egyptian gessoes have shown that they usually consist of a calcium carbonate or calcium sulphate filler mixed with an organic binder.[2] Animal glues, originating from different animal sources, were commonly used as binders in gesso.[3]

Aston *et al.* noted that gesso is strictly speaking a term for gypsum plaster, although Egyptologists use it commonly to refer to whiting plaster composed of powdered limestone mixed with glue, which appeared as early as the 3rd Dynasty in Saqqara for mounting blue tiles.[4] Gänsicke confirmed that the term gesso is commonly used in the Egyptological literature to refer to calcium carbonate – based grounds, but compositions vary and gypsum – based grounds have been identified.[5] Single or multiple layers, with or without linen, were applied. Gale[6] mentioned that a thick gypsum plaster could be applied to timber to disguise the grain, but if the paint was to be applied, then gesso, made from whiting and gum, was used as a foundation. Stein and Lacovara[7] identified a thick calcium carbonate layer that was covered with a thin layer of gypsum as a colouring layer.

It is a bit difficult to set a certain trend for the composition of the preparation layers, because of the diversity of polychrome wood in ancient Egypt, so far it is not clear which material was employed as a coating on wooden objects during the different periods, and the fact that wooden coffins were reused in many cases causes further complications in setting a certain rule for the use of materials. It has become clear from previous research, though that since the 18th Dynasty calcium carbonate was frequently used.

Assessment of wood, preparation layer and colouring layers in archaeological polychrome wooden artefacts, that form a large percentage of our organic cultural heritage, are always the first step of the documentation prior to any treatment. Decaying factors usually include biological, chemical and mechanical factors that affect an object during its burial or after its excavation. Environmental parameters, biological and non-biological, that contribute to the degradation of various types of wood in cultural heritage objects have often been studied and discussed, but how the materials used in making any artistic object affected each other has rarely been considered.

A few studies indicated that chemical hydrolysis was most likely responsible for some degradation patterns observed in the wood structure, when the wood is in contact with limestone, gesso, or

* The Authors would like to thank Dr. Mahmoud Sayed, South Valley University, for providing all the wood samples.

1 Stein and Lacovara 2010.
2 Hatchfield and Newman 1991.
3 Newman and Halpine 2001.
4 Aston *et al.* 2000.
5 Gänsicke 2010.
6 Gale *et al.* 2000.
7 Stein and Lacovara 2010.

various minerals over long periods of time.[8] These patterns include cell wall deterioration beginning at a cell lumina level and progressing into the secondary wall, as well as the organized microfibrillar structure being converted into an amorphous mass of residual material.[9]

The aim of this research was to assess causes of wood deterioration from a totally different perspective, in order to understand the 'initial' decay mechanism in polychrome wooden objects. Wood components start to degrade after their exposure to any 'foreign or added' material, a fact that has often been overlooked during the assessment of decay. The process of covering the wood with a white preparation layer could be considered the first stage of decay in wood, and that explains why SEM micrographs of wood lying directly beneath this layer clearly show signs of deterioration, whereas other parts of wood within the same object may not show the same type of decay.

Materials and Methods

Wooden supports

The most widely used native wood in Ancient Egypt was *Ficus sycomorus* (sycomore fig). *Tamarix* sp. (tamarisk wood) was less widely used, and rarely were large objects made of either *Acacia* sp. or *Ziziphus spina-christi*.[10] According to the facts in literature that mentioned the different types of wood used in polychrome funerary furniture three types of wood were chosen for this study; namely sycomore fig wood, tamarisk and acacia. Wood blocks (seven of each type, approx. 10x10x2cm) had been cut and left to be seasoned naturally in Luxor, South of Egypt, where the weather conditions are relatively dry and hot.

Preparation layers

For the experimental part of this research the wood was covered with a layer similar to that found in a large number of ancient Egyptian coffins. It is mentioned in literature that the preparation layer in most of the identified coffins was composed of calcium carbonate, but the presence of gypsum has been documented, and cannot be overlooked.

For this research commercially available calcium sulphate ($CaSO_4 \cdot 2H_2O$), referred to in most of the literature as gypsum, and lime plaster or calcium carbonate ($CaCO_3$), referred to in most of the literature as chalk, were used. The three wood types were coated, each separately, with a thin layer of one of the following six preparation layers:

a. Chalk mixed in water.
b. Chalk mixed in a previously prepared animal glue solution (1 glue : 15 water v/v), after priming the wood surface with animal glue.
c. Gypsum mixed in water.
d. Gypsum mixed in a previously prepared animal glue solution (1 glue : 15 water v/v), after priming the wood surface with animal glue.
e. Chalk mixed in water, to which a small amount of gypsum was added (ca. 85% chalk and 15% gypsum).
f. Chalk mixed in a previously prepared animal glue solution, to which a small amount of gypsum was added (ca. 85% chalk and 15% gypsum), after priming the wood surface with animal glue.

The composition of the six preparation layers was chosen in a way that would make it possible to study the 'initial deteriorating effect' of both chalk and gypsum separately or within a composite material on the three wood types. The blocks were left to dry in the open air and then stored for almost two years in normal Cairo weather conditions (naturally aged).

8 Obst *et al.* 1991; Blanchette *et al.* 1991a; Blanchette *et al.* 1994.
9 Blanchette *et al.* 1991b.
10 Davies 1995.

Sampling

It was necessary to carefully remove the preparation layer and take a sample of the wood that lay directly beneath. Three types of preparation layers that did not contain animal glue were analysed using XRD, in order to record their mineral composition.

For each wood type a 'control sample' and six treated samples were collected for SEM and FT-IR analysis.

Analysis and Investigation Methods

- X-Ray Diffraction (XRD)
  The mineral composition of the preparation layers and its percentage was confirmed using a Philips Analytical X-Ray B.V.; PC-APD diffraction software; diffractometer type: PW 1840, with a Cu tube anode; generator tension 40 KV and generator current 25 MA. The CuKα radiation consists of Kα1 (0.154056 nm) and Kα2 (0.154439 nm) components. Scans were obtained from 5 to 60 degrees 2θ in 0.03 degree steps for 0.3 seconds per step. Three samples from the preparation layers, one composed of chalk, one composed of gypsum and one composed of a mixture of both chalk and gypsum were analyzed and the minerals that they were composed of were identified.
- Scanning Electron Microscopy (SEM)
  A total of 21 wood samples were studied using scanning electron microscope (SEM). The samples were mounted on aluminium stubs with double-sided cellophane tape. After gold coating using a Polaron sputter coater, the samples were examined by SEM (JEOL scanning electron microscope JXA-840A).
- Fourier Transform Infra Red Spectroscopy (FT-IR)
  For monitoring the chemical changes and modifications which occurred in the wood due to the chemical effect of the adherent preparation layers that had remained in direct contact with the wood for almost two years, 21 samples were analysed with an FT-IR Spectrometer (Model 6100 Jasco, Japan). Spectra were obtained in the transmission mode with TGS detector using KBr method and represent (2mm/Sec) co -added scans at the spectral region ranging from 4000 to 400 cm^{-1} with resolution of 4 cm^{-1}. The peaks with the maximum intensities in all the FT-IR figures were normalized at the same value.

Results and Discussion

The XRD results confirmed that the newly prepared layers were composed of either pure calcium carbonate or gypsum. The layer that was composed of a mixture of chalk and gypsum contained 86% chalk and 14% gypsum.

SEM was used to monitor the changes in the anatomical structure of the wood samples that had been covered with preparation layers. The results show clearly that the surface of wood which adheres directly to the preparation layers undergoes distinct chemical and mechanical changes according to the composition of these layers.

Large differences between the two main wood components of the three wood types had been identified quantitatively in previous research[11] as shown in Table 1, and that explained the vast differences in the chemical bonds seen in the FT-IR spectra of the wood types (Fig. 1 and Table 2).

Table 1. Lignin and Carbohydrate percentage and ratio in Ficus, Tamarix and Acacia wood

Wood type	Lignin %	Carbohydrates %	Lignin : Carbohydrates
Ficus	30	39	0.77
Tamarix	19	60	0.32
Acacia	35	28	1.25

11 El Hadidi 2003.

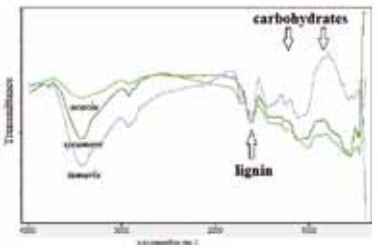

Fig. 1. FT-IR spectra of the three wood types clearly indicating the vast differences in the relative intensities between typical carbohydrate bands in the regions between 1320 - 1375, 880 - 1050 and the lignin band at around 1600 (© Faculty of Archaeology, Cairo University).

Table 2. FT-IR bands in the three wood types

Ficus	Tamarix	Acacia	Bands
3430	3423	3442	strong hydrogen bonded (O-H) stretching absorption
2921	2924	2921	C-H stretching absorption around 2997
	1737	1729	Around 1738-1734cm^{-1} for unconjugated C = O in xylans (hemicellulose)
1618	1617		1650cm^{-1} for absorbed O-H and conjugated C-O
	1609	1599	1596cm^{-1} and 1505-1511cm^{-1} for aromatic skeletal in lignin
	1456		1462cm^{-1} and 1425cm^{-1} for C-H deformation in lignin and carbohydrates
1424	1428	1420	
1377	1377	1376	1375cm^{-1} for C-H deformation in cellulose and hemicelluloses
1322	1335	1324	1330-1320cm^{-1} for C-H vibration in cellulose and C_1-O vibration in syringyl derivatives
1260	---		1268cm^{-1} for guaiacyl ring breathing, C-O stretch in lignin and for C-O linkage in guaiacyl aromatic methoxyl groups
	1247	1250	1244cm^{-1} for syringyl ring and C-O stretch in lignin and xylan
absent in all three			1158cm^{-1} for C-O-C vibration in cellulose and hemicelluloses
1114	1117	---	1122cm^{-1} for aromatic skeletal and C-O stretch
1029	1047	1021	1048cm^{-1} for C-O stretch in cellulose and hemicellulose
885	888	893	898cm^{-1} for C-H deformation in cellulose

The main lignin and carbohydrate bands in the three wood types were recorded, according to Pandey and Pitman[12] 2003, before and after covering the wood with all six preparation layers, in order to note the chemical changes that occurred in the wood samples. The bands of both chalk and gypsum were taken into consideration while studying the FT-IR results.[13] The appearance or disappearance of bands in every wood type was checked separately and the transmittance trends of the bands in the FT-IR spectra were compared (Tables 3-5).

Lignin and Carbohydrate bands in the three wood types

- Lignin bands

One clear aromatic skeletal band was evident in all three wood types, but they were recorded in different positions ranging from 1599 – 1618. The bands at around 1505 were absent in all three cases. A band at 1261 was evident only in sycomore fig wood and the band at around 1244 was present in tamarisk and acacia. The band at around 1122 was present in sycomore and tamarisk, but absent in acacia.

- Carbohydrate bands

The hemicellulose band at 1738 was absent in sycomore, but was present in tamarisk and acacia

12 Pandey and Pitman 2003.
13 Genestar 2002.

with a slight shift. The O-H groups of cellulose and hemicelluloses were only present in tamarisk, whereas, the CH_2 of cellulose and hemicelluloses were present in sycomore and acacia. The C-O-C vibration in cellulose and hemicelluloses at 1158 were absent in all three wood types. The rest of the carbohydrate bands were present in all three types, with a shift in some cases.

The effect of treatments on the main wood components

- Samples covered with chalk-based preparation layers

Numerous cracks and fissures were developed within the secondary wall, especially S_3 layer, showing evidence of lignin degradation. The degradation caused a delamination of wood cells and sustained cracks and fissures appeared within the secondary wall of the cells, as well as a partial loss of cells in the samples covered with chalk and glue (Fig. 2). The fractured surface of wood cells in the samples covered with preparation layer based on chalk showed large voids, loss in cell corners and separation of the cells due to loss of middle lamella layers, as a result of the chemical deterioration, that caused adjacent cells to separate from each other. Cell separation appeared most clearly in the acacia wood samples (Fig. 2 e-f), where partial deterioration of the pits appeared in the form of an increase in openings and unevenness. Additionally a parallel series of separations occurred within the cell wall layers, and presumably all layers of the cell wall, including the cellulose rich secondary wall layers were affected by the chemical reaction.

The alkaline effect of chalk is evident in the FT-IR spectra (Fig. 3). The strong transmittance seen in the lignin bands in the FT-IR spectra of all three wood samples became either weaker or disappeared in the wood samples covered with chalk. The main carbohydrate bands showed relatively stronger transmittance after treatment in comparison to the untreated wood samples.

Acacia wood, which is rich in lignin, showed most clearly the effect of chalk, where the lignin band decreased and the carbohydrate bands increased greatly relative to each other. The chemical effect of chalk even reached an extent that some of the lignin and hemicellulose bands disappeared.

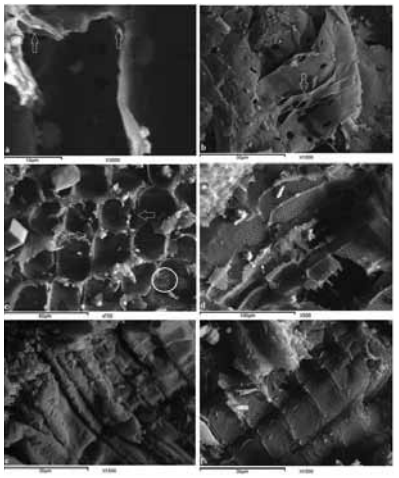

Fig. 2. SEM micrographs of wood samples covered with chalk preparation layers showing uneven erosion of cell wall corners, loss of middle lamella region as well as cracks and fissures within the secondary wall; (a) Sycomore + chalk, (b) Sycomore + chalk + glue, (c) Tamarisk + chalk, (d) Tamarisk + chalk + glue, (e) Acacia + chalk, (f) Acacia + chalk + glue (© Faculty of Archaeology, Cairo University).

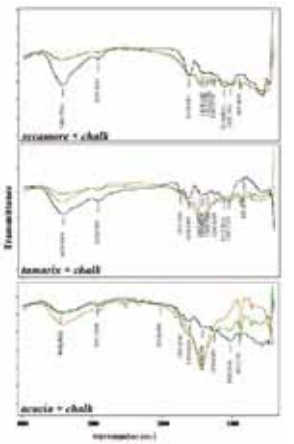

Fig. 3. FTIR spectra of three types of wood after treatment with chalk showing the alkaline effect on the lignin bands, which decreased in intensity. It was most clearly seen in the case of acacia, which had the highest lignin content. (black spectra = wood; green = wood treated with chalk; brown = wood treated with chalk + glue) (© Faculty of Archaeology, Cairo University).

- Samples covered with gypsum-based preparation layers

Wood samples covered with gypsum- based layers showed gradual degradation and erosion in cell wall carbohydrates, resulting in erosion and loss of the cell walls partially and completely (the mass loss increased), in addition to collapse of the wood structure, especially in tamarisk samples as extensive decay and erosion occurred in wood cells. Cracks and separations were also evident in secondary wall regions due to erosion of cell wall layers (Fig. 4).

Gypsum is acidic, and while setting causes an exothermic reaction. The chemical effect of the gypsum- based layer is evident in Fig. 5, where the gypsum mainly affected the carbohydrates, leaving prominent lignin bands. The effect of gypsum is best seen in the tamarisk sample, due to its richness in carbohydrates. Here the relative intensities of carbohydrate bands to lignin bands, changed drastically after treatment with gypsum. Additionally some of the carbohydrate bands disappeared.

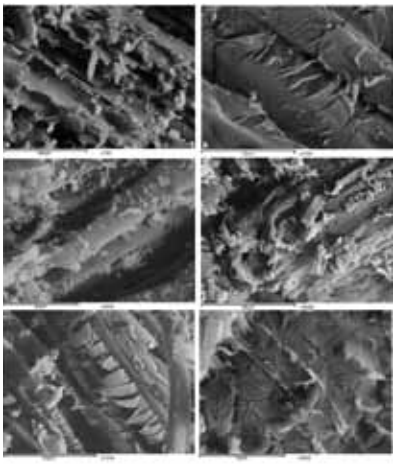

Fig. 4. SEM micrographs of wood samples covered with gypsum preparation layers showing completely eroded parts of the cell wall. Separations, cracks and fissures occurred within the cell wall layers; (a) Sycomore + gypsum, (b) Sycomore + gypsum + glue, (c) Tamarisk + gypsum, (d) Tamarisk + gypsum + glue, (e) Acacia + gypsum, (f) Acacia + gypsum + glue (© Faculty of Archaeology, Cairo University).

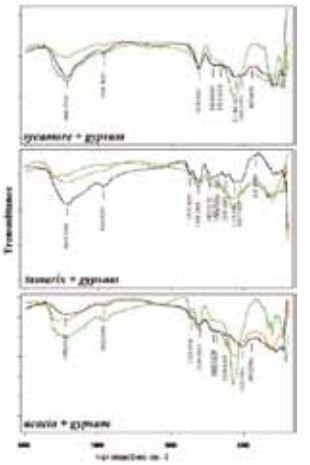

Fig. 5. FTIR spectra of three types of wood after treatment with gypsum, showing the acidic effect on wood carbohydrate bands which decreased in intensity. It was most evident in tamarisk wood, which had the highest carbohydrate band. The extremely broad bands in the region between 600 and 800 and around 1100 in the sycomore fig wood and acacia samples are attributed to the gypsum bands in addition to the wood carbohydrates. (black spectra = wood; green = wood treated with gypsum; brown = wood treated with gypsum + glue) (© Faculty of Archaeology, Cairo University).

- Samples covered with preparation layers based on a mixture of chalk and gypsum

The preparation layers based on a mixture of chalk and gypsum degraded wood surface extensively, especially in the presence of glue. The overall effect is that the wood loses its integrity. The samples exhibited a progressive erosion and loss in the middle lamella region and parts of the cell wall layers due to the chemical attack leading to the gradual breakdown of the wood cells which became easily fragmented. The cell wall layers are disrupted and dispersed due to the extensive degradation, and delamination in cell wall layers was observed (Fig. 6).

The dual effect of both materials, alkalinity of chalk and acidity of gypsum, lessened the alkalinity of chalk and the exothermic effect of gypsum, because gypsum was added to the previously prepared chalk mixture. Chalk percentage in comparison to that of gypsum in the layer was much higher, and this gave an effect similar to that given by the chalk – based layer, with a decrease in intensities. That

did not prevent the disappearance of some of the hemicellulose and lignin bands in the different types of wood (Fig. 7).

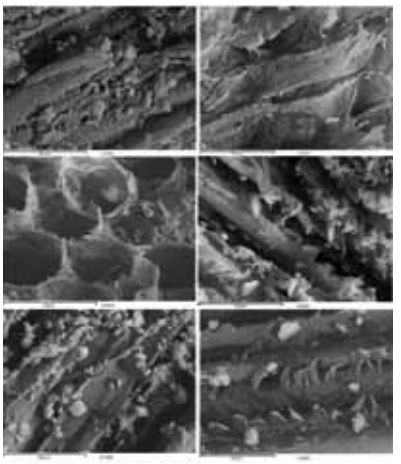

Fig. 6. SEM micrographs of wood samples covered with preparation layers based on a mixture of chalk and gypsum showing that the gradual breakdown of the wood cells resulted in that cells became easily fragmented, as well as the cell wall layers are disrupted and dispersed due to the extensive degradation; (a) Sycomore fig wood + chalk + gypsum, (b) Sycomore fig wood + chalk + gypsum + glue, (c) Tamarisk + chalk + gypsum, (d) Tamarisk + chalk + gypsum + glue, (e) Acacia + chalk + gypsum , (f) Acacia + chalk + gypsum + glue (© Faculty of Archaeology, Cairo University).

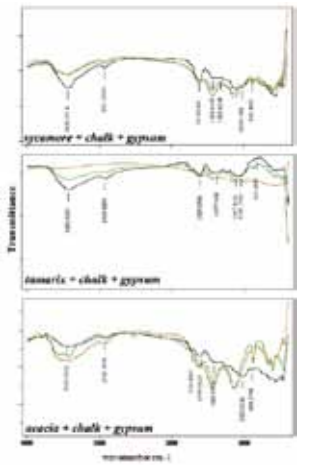

Fig. 7. FTIR spectra of three types of wood after treatment with chalk and gypsum showing the dual effect of both minerals. The alkaline effect of chalk on lignin was stronger than the acidic effect of gypsum. (black spectra = wood; green = wood treated with chalk + gypsum; brown = wood treated with chalk+ gypsum + glue) (© Faculty of Archaeology, Cairo University).

- Samples covered with preparation layers containing animal glue

SEM results indicated that the presence of animal glue in the preparation layers increases the mechanical changes in the cell wall layers. The cracks and fissures within the secondary wall regions of the cells, as well as separation, erosion and loss of cells occurred aggressively in the samples covered with preparation layers containing glue (Figs. 2, 4, 6b, 6d, 6f).

The FT-IR spectra clearly indicated that the animal glue did not affect the chemical bands of either the carbohydrates or lignin. The most obvious changes were mainly noted in the bands of the minerals as follows:

Minute differences can be seen in the cases of sycomore fig wood and tamarisk treated with chalk and chalk and glue. After treating acacia with chalk and water, the bands belonging to the calcium carbonate at around 1409 and 872 were relatively strong, in addition to the area in between. The addition of glue to chalk on acacia wood resulted in even stronger calcium carbonate bands.

After treating the wood with gypsum the main sulphate band around 1150 (very broad) and the two bands in the 600 region showed strong transmittance, the intensity of these bands decreased with the use of animal glue. In tamarisk the gypsum bands were not as strong as in the other two cases.

The spectra of wood treated with a mixture of chalk and gypsum showed slight differences between the mixtures that were with or without glue. The strangest spectra was obtained in the case of the layer containing glue on tamarisk wood, the intensities of the major wood bands in the region between 1800 and 800 were relatively small and weak, but a clear logical explanation is difficult to find.

Discussion

Blanchette suggested that differences in the appearance of the surface deterioration occurring in Egyptian wood, which was taken from ancient tombs, were most likely due to the much longer time of burial, to the more direct contact with alkaline substances, or to the different types of minerals.[14]

To understand the mechanism of decay it was necessary to start by looking closely at the components of the three wood types. The quantitative analysis of carbohydrate and lignin content had been determined in previous research,[15] according to which the ratio of lignin: carbohydrates in the three chosen angiosperms were calculated. The vast differences in table 1 were noticeable in the FT-IR spectra (Fig. 4), and it would have been interesting to calculate the average relative intensities of lignin peaks against carbohydrate peaks, but that was not possible, because Pandey and Pitman[16] depended in their calculations on the lignin peaks at around 1510 cm^{-1}, which were were not detected in all three wood types.

This study proved that differences in the appearance of the surface deterioration caused by chemical attack are due to the different types of minerals contained in the preparation layers, in addition to the chemical composition of the wood type.

SEM results showed a general weakening of the wood cell wall composition and separations along the fibril orientation of the cell walls suggesting a form of chemical erosion, due to the various components of preparation layers, similar to that caused by salts or minerals. There were significant differences in the decay patterns of chemical attack between the three types of wood, due to two main reasons. The first one being the differences of lignin and carbohydrate bands in the three angiosperms, and the second one the different pH values of the preparation layers; i.e. chalk being alkaline and gypsum being acidic.

The data obtained from both the SEM and FT-IR results were almost compatible. The chemical attack of the minerals caused defibration of the entire wood surface generally. SEM results showed loss the middle lamellae region especially in cell corners as well as between cells which caused separations between cells in addition to, fissures within the secondary wall. These decay patterns presumably are due to the fact that chalk degrades lignin more readily than carbohydrates.

Acids degrade carbohydrates and modify lignin.[17] FT-IR results showed that gypsum affected, in addition to the main carbohydrate bands, the C_1-O vibration in syringyl derivatives aromatic skeletal and C-O stretch in some of the cases. SEM showed separation between and within the cell walls in addition to cracks and fissures which were developed within the secondary wall, which can be explained as a consequence of the depolymerisation of lignin polymers throughout the cell wall without a considerable loss of lignin. This can be observed in the weakening of the cell walls as well as and partial loss of the cells due to the gradual degradation of cell walls. Additionally, the data showed that the presence of chalk and gypsum mixture in the layer caused severe deterioration of the wood surface, due to the combined effect of both chalk and gypsum.

It was obvious from SEM micrographs that gesso crystals were deposited on the surface, between cells and within cell walls. In areas where gesso crystals accumulated, a total hydrolysis of wall material was evident. SEM results also indicated that samples covered with preparation layers containing glue suffered more deterioration than those without glue which means that glue significantly increases mechanical degradation. This might be explained due to the contraction of glue after drying of the preparation layers. Additionally, glue makes the preparation layers more adherent to the wood surface which may increase the chemical deterioration.

The presence of preparation layers causes serious damage to wood and accelerates the rate of

14 Blanchette 2003.
15 El Hadidi 2003.
16 Pandey and Pitman 2003.
17 Blanchette *et al.* 1991a; Blanchette *et al.* 1994.

degradation, as they result in water absorption if humidity and temperature are not controlled. This explains why the wood samples in this research suffered severe deterioration in a short period of time.

Conclusion

Effects of preparation layers on the anatomical structure and chemical composition of three types of wood were investigated. Although the data obtained from both the SEM and FT-IR techniques were mostly compatible, it is useful to note that sometimes there are changes in the chemical composition of wood observed using Infrared Spectroscopy, that do not appear in the anatomical structure. The results indicated that preparation layers cause serious damage to the adjacent wood surface. The patterns and the rate of degradation of wood covered with chalk- and gypsum-based layers differ according to the chemical composition of the layer which can be maximized if the layer contains both minerals. The importance of analysing the different layers which were used in the past to cover the wood surface must be emphasized before deciding to treat an object. The fact that coffins were reused should also be put into consideration, because this would mean that the wooden supports in the case of reuse would be re-exposed to chemical deterioration. Further research is needed to assess the effects of the preparation layers on other commonly used types of wood. That may help explain the damage that occurs if the wood is stored or exhibited in uncontrolled conditions, especially high relative humidity.

Understanding the condition of wood covered with preparation layers would enable conservators to plan and determine appropriate conservation procedures as well as selecting or developing treatment materials and methods applied on the outer layers of polychrome wood. It has always been a priority to treat the polychrome layers, due to important information that it contains. The wood carrying all the valuable data is always consolidated by default during the treatment of the upper layers, but the suitability of polymers to the wooden panel may not often be considered. That is a point of future research, which may reduce the risk of losing historically important artefacts.

Table 3. The changes in chemical bands that occurred in Ficus sycomorus

Ficus	Ficus + Chalk	Ficus + Chalk + glue	Ficus + Gypsum	Ficus + Gypsum + glue	Ficus + Chalk + gypsum	Ficus + Chalk + gypsum + glue	Bands according to literature
3430	3420	3430	3429	3456	3422	3432	Strong hydrogen bonded (O-H) stretching absorption
2921	2980	2921	2922	2920	2921	2928	C-H stretching absorption around 2997
Absent							1738-1734 cm^{-1} for unconjugated C = O in xylans
			1720				C=O stretching band at 1720 is due to the acidic effect of gypsum
1618	---	---	1624	1625	1617	1625	Conjugated C=O stretching
---	1589	1590	---				1596 cm^{-1} and 1505-1511 cm^{-1} for C=C stretching vibration in aromatic ring in lignin aromatic skeletal in lignin
1424	1422	1414	1428	---	1429	1430	1462 cm^{-1} and 1425 cm^{-1} for C-H deformation in lignin and carbohydrates
1377	Disappeared	Disappeared	1368	1382	Disappeared	Disappeared	1375 cm^{-1} for C-H deformation in cellulose and hemicelluloses
1322	Disappeared						1330-1320 cm^{-1} for C-H vibration in cellulose and C_1-O vibration in syringyl derivatives
1261	1271	1273	Disappeared				1268 cm^{-1} for guaiacyl ring breathing, C-O stretch in lignin and for C-O linkage in guaiacyl aromatic methoxyl groups
Absent		1235	Absent				1244 cm^{-1} for syringyl ring and C-O stretch in lignin and xylan
Wood bands Absent	1152	Absent	1147	Absent	1146	Absent	Vibration frequencies of sulphate
1113	1129	Disappeared	1104	1121	Disappeared	Disappeared	1122 cm^{-1} for aromatic skeletal and C-O stretch
1029	Disappeared	1009	Disappeared	1012	1024	1147	1048 cm^{-1} for C-O stretch in cellulose and hemicellulose
885	--- 876	--- 876	--- ---	--- 884	--- 876	--- 873	898 cm^{-1} for C-H deformation in cellulose Band at 875 cm^{-1} is due to CO_3^{2-} group of chalk.

Comment:
Lignin:
A strong band at 1618, which was evident in the wood sample, remained prominent in four cases; after treatment with gypsum, gypsum + glue, chalk + gypsum and chalk + gypsum + glue. This band was shifted to around 1590 after treatment with chalk and chalk + glue. Lignin band at 1268 disappeared after treatment with layers containing either gypsum or chalk + gypsum (with or without glue). The aromatic skeletal and the C-O stretch at 1122 were originally shifted in the wood sample and remained prominent after treatment with chalk, gypsum, gypsum + glue.
Carbohydrates:
The carbohydrate bands at 1375 disappeared after treatment in the wood treated with chalk and chalk + gypsum, but was slightly shifted in the case of gypsum. The bands at 1322 disappeared after all six treatments. The carbohydrate band at 1158 was not evident in the wood sample, but a band relating to gypsum became evident after treatment with gypsum and chalk + gypsum, with and without glue. The carbohydrate band at 1048 was shifted in the wood sample, and disappeared after treatment with chalk, gypsum and chalk + gypsum + glue.

Table 4. The changes in chemical bands that occurred in Tamarix sp.

Tamarix	Tamarix + Chalk	Tamarix+ Chalk + glue	Tamarix + Gypsum	Tamarix+ Gypsum + glue	Tamarix + Chalk + gypsum	Tamarix+ Chalk + gypsum + glue	Bands according to literature
3423	3421	3429	3434	---	3413	3484	Strong hydrogen bonded (O–H) stretching absorption
2924	2924	2926	2926	2929	2926	2928	C–H stretching absorption around 2997
---	---	1798	---	---	---	---	Band at 1798 cm^{-1} is due to CO_3^{2-} group of chalk.
1737	1728	Disappe-ared	Disappe-ared	Disappe-ared	1734	Disappe-ared	1738=1734 cm^{-1} for unconjugated C = O in xylans (hemicellulose).
---	---	---	1623	1627	1620	1619	Conjugated C=O stretching
1609	1578	1591	---	---	---	1580	1596 cm^{-1} and 1505-1511 cm^{-1} for aromatic skeletal in lignin
1456 1428	1423	1426	Disappe-ared	Disappe-ared	1431	1421	1462 cm^{-1} and 1425 cm^{-1} for C–H deformation in lignin and carbohydrates
1377	Disappeared						1375 cm^{-1} for C–H deformation in cellulose and hemicelluloses
1335	1330=1320 cm^{-1} for C–H vibration in cellulose and C_1–O vibration in syringyl derivatives						
Absent							1268 cm^{-1} for guaiacyl ring breathing, C–O stretch in lignin and for C–O linkage in guaiacyl aromatic methoxyl groups
1247	Disappeared						1244 cm^{-1} for syringyl ring and C–O stretch in lignin and xylan
Wood bands Absent	1158	Absent	1151	1154	Absent	Absent	Vibration frequencies of sulphate
1117	1122	1128	Disappe-ared	Disappe-ared	1126	Disappe-ared	1122 cm^{-1} for aromatic skeletal and C–O stretch
1047	Disappe-ared	1028	Disappe-ared	1015	Disappe-ared	1003	1048 cm^{-1} for C–O stretch in cellulose and hemicellulose
888	--- 875	--- 874	Disappe-ared ---	898 ---	--- 877	--- 875	898 cm^{-1} for C–H deformation in cellulose. Band at 875 cm^{-1} is due to CO_3^{2-} group of chalk.

Comment:
Lignin:
Aromatic skeletal in lignin band at 1596 was evident in the wood sample (with a shift), after treatment with chalk, chalk + glue, and chalk + gypsum + glue, but may have merged with the gypsum band in all other samples; whereas the aromatic skeletal and the C-O stretch at 1122 was only evident before and after treatment with chalk (with and without glue) and chalk + gypsum.
Carbohydrates:
Main hemicelluloses band at around 1730 was present in tamarisk before and after treatment with chalk and chalk + gypsum, showed a large shift after treatment with chalk + glue due to CO_3^{2-} group of chalk at 1798, but disappeared after treatment with gypsum, gypsum + glue and chalk + gypsum + glue. The carbohydrate band at 1377, the band at 1335 and the band at 1247 were only present in the case of tamarisk wood, but disappeared after all six treatments. The carbohydrate band at 1158 was not evident in the wood sample and wood treated with chalk + glue, chalk + gypsum (with and without glue), but became evident after treatment with gypsum, with and without glue. The carbohydrate band at 1047 was present in the wood sample and after treatments which contained glue, but disappeared in the rest of the treatments.

Table 5. The changes in chemical bands that occurred in Acacia sp.

Acacia	Acacia + Chalk	Acacia + Chalk + glue	Acacia + Gypsum	Acacia + Gypsum + glue	Acacia + Chalk + gypsum	Acacia + Chalk + gypsum + glue	Bands according to literature
3442	3436	3415	---	3409	3414	3416	Strong hydrogen bonded (O-H) stretching absorption
2921	2938	2970	2925	2945	2973	2930	C-H stretching absorption around 2997
---	---	1797	---	---	1797	1794	Band at 1797 cm^{-1} is due to CO_3^{2-} group of chalk.
1729	1723	---	1732	Disappeared	---	---	1738=1734 cm-1 for unconjugated C = O in xylans (hemicellulose).
---	---	---	1623	1626	1621	1627	1650 cm^{-1} for absorbed O-H and conjugated C-O
1599	1583	---	---	1535	---	---	1596 cm^{-1} and 1505-1511 cm^{-1} for aromatic skeletal in lignin
1420	1423	1424	1431	1409	1430	1432	1462 cm^{-1} and 1425 cm^{-1} for C-H deformation in lignin and carbohydrates
1376	Disappeared		1375	Disappeared			1375 cm^{-1} for C-H deformation in cellulose and hemicelluloses
1324	Disappeared		1320	Disappeared			1330=1320 cm^{-1} for C-H vibration in cellulose and C_1-O vibration in syringyl derivatives
Absent							1268 cm^{-1} for guaiacyl ring breathing, C-O stretch in lignin and for C-O linkage in guaiacyl aromatic methoxyl groups
1250	Disappeared						1244 cm^{-1} for syringyl ring and C-O stretch in lignin and xylan
Wood bands Absent	1163	1165	1150	1144	1147	1149	Vibration frequencies of sulphate
	1118	Absent					1122 cm^{-1} for aromatic skeletal and C-O stretch
1021	1031	Disappeared					1048 cm^{-1} for C-O stretch in cellulose and hemicellulose
893	--- 876	--- 874	--- ---	--- 881	--- 875	--- 876	898 cm^{-1} for C-H deformation in cellulose. Band at 875 cm^{-1} is due to CO_3^{2-} group of chalk.

Comment:

Lignin:

Aromatic skeletal in lignin band at 1596 was evident in the wood sample and after treatment with chalk, disappeared after treatment with chalk + glue, but may have merged with the gypsum band in all other samples. The aromatic skeletal and C-O stretch at 1122 appeared only after treatment with chalk.

Carbohydrates:

The main hemicellulose band at around 1730 was present in acacia wood before and after treatment with either chalk or gypsum, but disappeared after treatment with gypsum and glue. This band may have either merged or showed a shift with CO_3^{2-} group of chalk at 1797 after treatment with chalk + glue, chalk + gypsum and chalk + gypsum + glue. The carbohydrate band at 1375 and the band at 1324 were only present prior treatment and after treatment with gypsum, but disappeared in the rest of the cases. The bands at 1250 disappeared after all six treatments.

The carbohydrate band at 1158 was absent in the wood sample, but bands around the same region appeared after all 6 treatments. The carbohydrate band at 1048 was shifted in the wood sample and after treatment with chalk, but disappeared in the rest of the treatments.

Photo credits

Photos © Governatorato SCV, Direzione dei Musei
Images and Rights Office: Rosanna Di Pinto, Filippo Petrignani
Secretary for Departments: Daniela Valci, Gianfranco Mastrangeli
Photographers: Pietro Zigrossi, Alessandro Bracchetti, Giampaolo Capone, Luigi Giordano, Danilo Pivato, Alessandro Prinzivalle
Photos R. Hiramoto: pp. 104, 216
Photos N. Crawford: pp. 211, 215

© The Fitzwillian Museum, Cambridge: pp. 522-527
© Arheološki Muzej in Zagreb (kind permission): pp. 552-555 (photo F. Beusan)
© Bibliotheca Alexandrina Antiquities Museum (photo C. Gerigk): p. 24 (fig. 4)
© Bolton Council from the collections of Bolton Museum: p. 479 (fig. 12)
© Boris Lipnitzki/Roger-Viollet/Archivi Alinari, Firenze: p. 562 (fig. 1)
© Castello del Buonconsiglio, Trento: pp. 271, 273-275
© Cl. Ghislaine Gendron, Musée Dobrée – Grand patrimoine de Loire-Atlantique: p. 130 (fig. 1A)
© Leeds Museums and Art Galleries (City Museum), UK: p. 80
© Liebieghaus Skulpturen Sammlung/Bormann: p. 81
© Musée d'art et d'histoire, Ville de Genève: pp. 252 (photo Y. Siza), 253 (photo B. Jacot-Descombes), 429 (fig. 6, inv. n. 012440, photo M. Aeschimann et B. Jacot-Descombes)
© Musée Testut Latarjet d'Anatomie et d'Histoire naturelle médicale, Lyon (kind permission): p. 131
© Museo del Vicino Oriente, Egitto e Mediterraneo, Sapienza University of Rome (photo M. Necci): pp. 407, 509
© Neuchâtel Museum of Ethnography, Switzerland: pp. 251 (fig. 2), 254, 507 (fig. 8)
© TAJAN: p. 130 (fig. 1C)
© The Cleveland Museum of Art: p. 25
© The Trustees of the British Museum: pp. 22-23, 26-27, 138, 139 (fig. 2), 141 (fig. 5), 309-315, 543-550
© University of Basel Kings' Valley Project: pp. 84-85 (fig. 2, drawing by T. Alsheimer), 86-87 (photo M. Kacicnik)
© Ville de Clermont-Ferrand – Collections du Musée Bargoin, cl. T. Mollard: p. 126 (fig. 3B)
Archives nationales de France, AF^{IV} 17240: p. 123
Bibliothèque nationale de France: p. 441 (fig. 8)
Brooklyn Museum (kind permission): p. 441 (fig. 7)
C2RMF (kind permission): pp. 172 (fig. 2, photo G. de Puniet; fig. 3, image by S. Pagès-Camagna), 173 (image by S. Pagès-Camagna)
Central Manchester University Hospitals NHS Foundation Trust (kind permission): pp. 54-55
Civici Musei di Storia ed Arte di Trieste (kind permission): pp. 318-322
Civico Museo Archeologico, Asti (kind permission): pp. 278-279, 281-285
Collection Muséum d'Histoire Naturelle de la Rochelle: pp. 114-119, 567 (fig. b)
Consiglio Nazionale delle Ricerche (kind permission): pp. 407-416
Courtesy of The Egypt Exploration Society: p. 37 (right image)
Courtesy of the Middle American Research Institute, Tulane University: pp. 329-333
Deutsches Archäologisches Institut Kairo (kind permission): pp. 452-453 (drawing by S. Michels), 457 (drawing by S. Fetler), 458-462
Éditions Musée du Louvre (kind permission): p. 428 (fig. 4)
Faculty of Archaeology, Cairo University (kind permission): pp. 202-205
Fondazione Museo delle Antichità Egizie di Torino (kind permission): pp. 92-95, 107 (figs. 8-9), 107 (fig. 8, photo N. Crawford; fig. 9, photo R. Hiramoto)
G. Schreiber (kind permission): pp. 464-470 (photo L. Mátyus)
Garstang Museum of Archaeology, University of Liverpool (kind permission): pp. 293-294 (figs. 1-3, photo by the authors of the essay)
Griffith Institute, University of Oxford: pp. 370-377, 430
Images by A. Tang (kind permission): pp. 212-213
KNH Centre for Biomedical Egyptology University of Manchester – Ancient Egyptian Animal Bio Bank Project, Central Manchester University Hospitals NHS Foundation Trust (kind permission): pp. 295-296 (photo C. Brassey), 297 (photo by the authors of the essay)
Kramskoy Voronezh Regional Art Museum (kind permission): p. 531 (fig. 3, photo S. Kupriyanov)
Kunsthistorisches Museum, Wien: pp. 106 (photo N. Crawford), 427

Lviv Historical Museum (kind permission): p. 539
Lviv Museum of the History of Religion (kind permission): p. 536
Medelhavsmuseet, Stockholm (kind permission): pp. 145-151 (photos A. Dodson)
Musée d'Archéologie Méditerranéenne, Centre de la Vieille Charité, Marseille (kind permission): pp. 126 (fig. 3A), 130 (fig. 1B)
Musée des Beaux-arts de Lyon (kind permission): pp. 126 (fig. 3C, photo A. Dautant), 221, 227-230 (photo A. Basset)
Musée du Louvre (kind permission): pp. 105 (fig. 3 photo N. Crawford), 171 (photo C2RMF/G. de Puniet), 174 (photo M. Garcia-Darowska), 175 (photo C2RMF/G. de Puniet and M. Garcia-Darowska), 176 (photo C2RMF/A. Chauvet), 177 (photo C2RMF/G. de Puniet and M. Garcia-Darowska)
Museo Civico Archeologico, Bologna (kind permission): pp. 362-367
Museo Egizio, Firenze (kind permission): pp. 105 (fig. 4, photo R. Hiramoto; fig. 5, photo N. Crawford), 107 (fig. 10, photo R. Hiramoto), 108 (photo R. Hiramoto), 180-182, 214, 217 (photos R. Hiramoto)
Museum Appenzell (kind permission): p. 251 (fig. 3)
Museum Gustavianum, Uppsala University (kind permission): pp. 342-345
Museum of Fine Arts, Budapest, 2017 (kind permission): pp. 261-269
National Museum in Warsaw (kind permission): pp. 156-162 (figs. 1, 3, 6, 7: photos Z. Doliński), (figs. 2, 4, 8: photos M. Doliński)
Odessa Archaeological Museum (kind permission): pp. 530, 531 (fig. 2) and 532 (photos N. Tarasenko)
Peter Brand (kind permission): p. 429 (fig. 5)
Photo © Musée du Louvre, dist. RMN-Grand Palais/Georges Poncet: pp. 79, 105 (fig. 2, photo R. Hiramoto), 442 (fig. 9)
Photo © Musée du Louvre, dist. RMN-Grand Palais/Les frères Chuzeville: pp. 71, 440 (fig. 5)
Photo I. Pridden (kind permission of the author of the essay): pp. 472-478
pmimage.ch/Neuchâtel Museum of Ethnography, Switzerland: pp. 503-507 (fig. 7), 508
Private Archives Haccius, courtesy of Bernard Haccius: p. 250 (photo F. Temporel)
Rijksmuseum van Oudheden, Leiden (kind permission): pp. 139 (fig. 3), 140, 419-424
Su gentile concessione del Comune di Padova, Assessorato Cultura e Turismo, Museo Archeologico – Musei Civici agli Eremitani: pp. 120-121
The Egyptian Museum, Cairo (kind permission): pp. 24 (fig. 3), 186, 188, 245-248, 346-348, 425, 428, 439 (fig.2)
The McManus: Dundee's Art Gallery & Museum (kind permission): pp. 32-36, 41-43
The Metropolitan Museum of Art, Gift of Mrs. G. W. Neville and Miss Cardwell, 1906 (kind permission): p. 479 (fig. 11)
The National Heritage Institute, Regional Historic Sites Management in Prague (kind permission): p. 440 (fig. 3)
The University of Manchester, Manchester Museum (kind permission): pp. 51-52, 53 (photo authors of the essay), 54-55
University of Dundee, Ninewells Hospital & Medical School Clinical Research Imaging Facility, CRIF (kind permission of L. Bidaut): p. 37 (left image)
Virginia Museum of Fine Arts, Richmond, lent by The Metropolitan Museum of Art (photo L. Boudreau): p. 440 (fig. 4)

Drawings by L. Di Ninno (kind permission of the author of the essay): p. 511 (fig. 2)
Drawings by L. Sist and I. Melandri (kind permission of the author of the essay): p. 513 (fig. 5)
Drawing by P. del Vesco and E. Taccola (kind permission of the author of the essay): p. 63 (fig. 1)

The images associated with each text, if not otherwise specified, have been provided by the respective authors, who assume any liability to third parties for their reproduction.
The Publisher is fully prepared to provide compensation due for any images for which it has not been possible to identify and locate the source.